Research Article

Theoretical Analysis of Heat Recovery Performance Air to Water of a Heat Pipe Heat Exchanger (HPHE)

Yuthapong Pakam and Thanakom Soontornchainacksaeng*
ES-MVC Research Center, Science and Technology Research Institute, Department of Mechanical and Aerospace Engineering, Faculty of Engineering, King Mongkut's University of Technology North Bangkok, Bangkok, Thailand

* Corresponding author. E-mail: tss@kmutnb.ac.th DOI: 10.14416/j.ijast.2016.11.007
Received: 14 February 2016; Accepted: 4 July 2016; Published online: 22 November 2016

Abstract
The purpose of this report is to analyze the heat recovery of the Heat Pipe Heat Exchanger (HPHE) by using ethanol as the working fluid. Heat pipe heat exchanger consists of 90 tubes were placed in staggered arrangement and inside the heat pipes was contained a screen wick and a working fluid. These pipes have been divided into three zones, consisting of evaporation zone, adiabatic zone, condensation zone, in each of zone, has a length of 500 mm, 100 mm and 500 mm, respectively. The mathematical models of HPHE which were simulated in MATLAB have the hot air flowing to evaporation zone with temperature range of 423.15 to 498.15K, and the cold water flowing to the condensation zone with a constant temperature of 303.15K. The ratio of hot air heat capacity rates to water heat capacity rates (C^*) are in the range of 0.50 to 1.50. The results showed that the C^* is 1.50 and the hot air temperature of 498.15K to be provided the best temperature for an exit cold water flow. The heat transfer coefficient of the hot air flowing to evaporation zone is 99.66 W/m^2.K as well as the heat flux of condensation zone is 23.226 W/m^2. Furthermore, at C^* = 0.50 and the hot air temperature inlet of 423.15K, showed the best effectiveness equal to 0.538. Therefore, the results of the HPHE simulation can be used to design for the boiler in distillery.

Keywords: Heat Pipe Heat Exchanger (HPHE), Heat recovery performance, Waste heat recovery, Screen wick, Staggered heat pipe

1 Introduction

In the manufacturing industry, HPHEs are usually used as a device to exchange heat between the hot fluid and cold fluid. The three main parts in HPHE are consists of the evaporation zone, adiabatic zone and condensation zone. A heat source is transferred to the heat pipes, which affects the working fluid in the heat pipes until it boils to vaporize then flowing up along the heat pipes on the top. Then, it releases the heat to cold fluid at the condensation zone. The working fluid condenses to liquid phase flowing via the wick and through to the evaporator zone to be heated again. The principle of the heat pipe is being applied for cooling and heat recovery system. About the considering research of HPHE, there were the in-line heat pipes arrangement to exchange heat of air to water. The heat pipes used water as working fluid. The theoretical results compared with the experimental results for the varying of the heat capacity rate of hot fluid per heat capacity rate of cold fluid (C_h/C_c) to evaluate the heat transfer rates, an effectiveness [1]. Therefore, the HPHE applied in high temperature nuclear reactor by a hot stream temperature inlet are 550–650°C and a cold stream temperature inlet are 14–18°C. The theoretical simulation model could be used for prediction the thermal

Please cite this article as: Y. Pakam and T. Soontornchainacksaeng, "Theoretical analysis of heat recovery performance air to water of a heat pipe heat exchanger (HPHE)," *KMUTNB Int J Appl Sci Technol*, vol. 9, no. 4, pp. 299–308, Oct.–Dec. 2016.

performance [2]. Also, the mathematic model using water as working fluid for air to water exchanging, It was studied for a hot air temperature range of 100–250°C, mass flow rates range of 0.05–0.14 kg/s, and a cool water is constant flowing of 0.08 kg/s. The model was able to predict the thermal performance [3]. Next, the energy recovery of HPHE is most important for evaluation. The mathematic model was simulated by a computer program to demonstrate for an air conditioning systems in the thermal performance as well [4]. Moreover, the temperature distribution use to evaluate the effectiveness which was analyzed with the numerical model to be created for a HPHE that focused on the changing of temperature distribution in each row [5]. Furthermore, the mathematical model utilize for heat recovery of HPHE by a ratio of inlet air per entering fresh air as shown the results that presents as mixing the fresh air and recovery air temperature of 40°C to be provided the best effectiveness is 0.48 [6]. However, the HPHE is not only be used in thermal system but also using in the air conditioning system such as the micro-fin copper tubes are studied the theory and experiments of HPHE used HFC134a and HFO1234ze(E) as the working fluid in the air conditioning system by exchanging the air to air. The results showed that HPHE was able to be applied [7]. Furthermore, there is also applied to the CPU. The effectiveness of finned U-shape heat pipe using in the cooling in order to find the ratio of the length of the evaporation zone to condensation zone in order to determine the total thermal resistance [8]. Also, for the vehicles, HPHE used for heat recovery from the internal combustion engines in which an air-to-water was used. The thermosiphon heat pipes are 2 meter-long steel was placed with staggered arrangement. Air temperature range were 100–250°C and air flow rate were 0.05–0.14 kg/s. The experiment results were compared with CFD model proved that tolerances was 10% [9]. Furthermore, applied for exchanging air's temperature in the engine with exhaust gas, the air was heated before entering the engine. The theoretical results were the same trend [10]. Also, the exhaust gas can be used for heat recovery in the internal combustion engines by the thermoelectric generators equipment by which was reduced the fuel usage and the emissions. Moreover, the mathematical model was able to assist in the design of HPHE by using R134a as the working fluid to reduce a moisture of inlet air which has temperature of 40–60°C and temperature of inlet air cold [11], [12]. In addition, there were the researches of heat transfer mechanism inside the heat pipe. Screen wick in heat pipe tested to know the phenomenon was provided the mathematic models to predict the dry out limit as well as screen wick was tested the maximum heat transfer rates [13]. Fortunately, HPHE is similar to the economizer, many of studying the energy recovery by economizer in the coal-fired power plant, flue gas desulfurizer system using exhaust gases [14], [15]. Next, the economizer using in the pasteurized dairy with exhaust gas to exchange with cold water [16]. The literature review found that the HPHE is useful for heat recovery. The research team would like to know the behavior of HPHE by using the suitable materials with much lower cost than copper as H. Zare Aliabadi *et al*. [1]. It's also should be to resist corrosion from an exhaust gas than steel. The research team chose stainless 304, and by using ethanol as the working fluid, and in addition to input the screen wick in heat pipe, including the analysis of heat pipe is staggered pipes arrangement. The mathematical model is created based on thermodynamics, fluid mechanics and heat transfer principles. In particular, this research is expected to have the information to be utilized for the further designation of the HPHE in order to using it as the heat exchanger equipment for industries.

2 Principle of HPHE

2.1 *Configuration of HPHE*

Design of the HPHE systems is conducted to recovery the wasted heat for increasing the water temperature. HPHE has the main components that consists of heat pipes bank, evaporation zone, adiabatic zone and condensation zone. The hot fluid flows at the evaporation zone and the cold fluid flows at the condensation zone as demonstrated in Figure 1. The design of the HPHE involves the temperature range, material, working fluid and screen wick. The HPHE which consists of a number of heat pipes can be placed either in the in-line or staggered arrangement. As the matter of facts, the surface area can be increased by applying the plate fins.

The principles of HPHE are shown in the Figure 1 which contained a bundle of heat pipes have the dimensions of 470×20×50 mm^3, are similar to the research of H. Zare Aliabadi *et al*. [1], the container

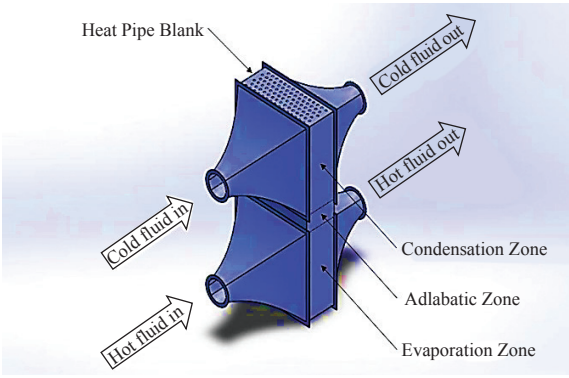

Figure 1: Schematic the configuration of HPHE.

material is a stainless 304, the screen mesh wick is made from a copper No.100 installed of 4 layers, by using ethanol as working fluid. The 90 heat pipes are installed to staggered arrangement with S_T = 30 mm, S_L = 30 mm and S_D = 42 mm. There is 6 rows of heat pipes and installed of 15 transverse heat pipes. The total length is 1100 mm; an evaporation zone's length is 500 mm, condensation zone's length is 500 mm and adiabatic zone's length is 100 mm. respectively. The outside diameter of heat pipes are 25.4 mm. The surface area is increased with plate fins have 4 mm. of thickness and installed distance of 300 fins/m.

2.2 *Testing conditions*

The hot air flows into the evaporation zone with the temperature range of 423.15–498.15K. The water transferred heat with a constant temperature is 303K, at condensation zone. The ratio of the heat capacity rates of the hot air to the heat capacity rates of the cold water (called capacity ratio) are in the range of 0.50–1.50. In fact, the mathematical models of fluids flowing via HPHE system have several differential equations from various physical principles. Firstly, the conservation of mass or continuity equation as shown in equation (1),

$$\vec{\nabla}.\left(\rho\vec{V}\right)=0 \tag{1}$$

Where $\vec{\nabla}$, ρ and $\vec{V}$ are the gradient operator, the density and the velocity field, respectively. The incompressible of Newtonian fluid flows through the element with steady state and constant density. This equation is used to calculate the mass flowrate via the surface area at evaporation zone and condensation zone. Next, the newton's second law of motion which is used to define the pressure field can be expressed as momentum equation as shown in equation (2),

$$\rho\left(\frac{\partial\vec{V}}{\partial t}+\left[\vec{V}.\vec{\nabla}\right]\vec{V}\right)=-\vec{\nabla}P+\rho\vec{g}+\mu\nabla^2\vec{V} \tag{2}$$

Where t, P, μ and $\vec{g}$ are the time, the pressure, the kinematic viscosity and gravity field, respectively. The energy equation is considered the internal energy, pressure-volume energy and heat conduction, but the external forces, potential energy and dissipation function are neglected. Thus, the energy equation gives the temperature distribution as equation (3).

$$\rho c_p\frac{DT}{Dt}=k\vec{\nabla}^2T+\frac{DP}{Dt} \tag{3}$$

The c_p, T and k are the specific heat, the temperature and the thermal conductivity, respectively.

2.3 *Heat transfer coefficient of HPHE*

Consideration on the average heat transfer coefficient of HPHE, the fluids flowing into the shell side, each of the heat pipes are the gathering of immersed flow and conduit flow [17]. The heat pipes are installed in staggered arrangement. Firstly, the maximum Reynold number is the function of maximum velocity, diameter, dynamic viscosity and density. The maximum velocity is the flowing of fluid via the smallest channel between two heat pipes at the same row [18], [19].

The S_D, S_L and S_T are the diagonal pitch, the longitudinal distance between two consecutive tubes and the transverse distance between two consecutive tubes, respectively. The maximum Reynold number, Re_{max}, is determined including the Prandtl number, Pr. Thus, the Nusselt number, Nu_{HPHE} can be determined from equation (4), as following,

$$Nu_{HPHE}=\frac{1+(n-1)f_A}{n}\left(\begin{array}{l}0.3+\\ \sqrt{\begin{array}{l}(0.664\sqrt{Re_{max}}Pr^{1/3})^2\\ +(\dfrac{0.037Re_{max}^{0.8}Pr}{1+2.433Re_{max}^{-0.1}(Pr^{2/3}-1)})^2\end{array}}\end{array}\right) \tag{4}$$

Where n is the number of heat pipe rows and f_A which is the arrangement factor is the function of

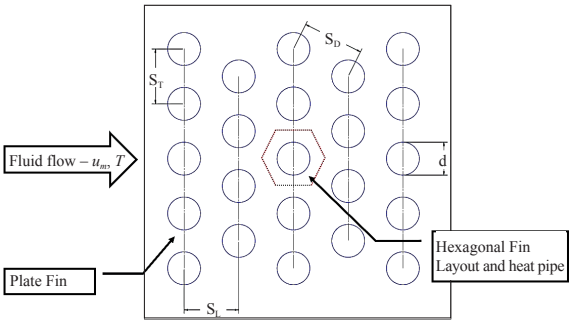

Figure 2: Schematic of fluid flowing via the plate fin and staggered heat pipes.

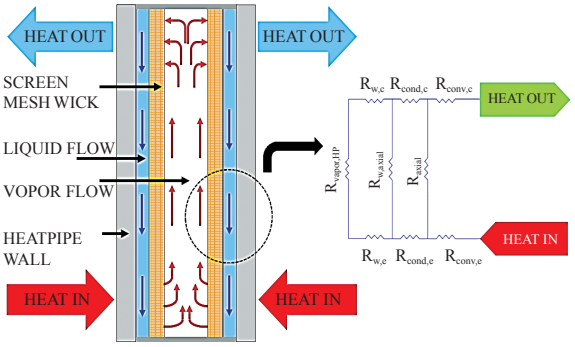

Figure 3: The working fluid within heat pipe.

the S_D, S_L, S_T and diameter, d. Thus, it can be determined from the equations (5) and (6), as following,

$$f_A = 1 + \frac{0.7\,b/a - 0.3}{\sigma^{1.5}(b/a + 0.7)^2} \tag{5}$$

Where the dimensionless pitches are $a = S_T/d$, $b = S_L/d$ and $c = S_T/2d$, respectively. Then, this equation can be used when $c < a/4$. and the void fraction, σ can be calculated from $\sigma = 1 - \pi/4a$ if $b \geq 1$ or $\sigma = 1 - \pi/4ab$ if $b < 1$

$$f_A + 1 + \frac{2}{3b} \tag{6}$$

This equation can be used when $c \geq a/4$. Also, the Nusselt number is available in the range of the maximum Reynold number $10 < Re_{max} < 10^5$ and the Prandtl number, $0.6 < Pr < 10^3$ [20]. In particular, the mean heat transfer coefficient, $\overline{h}$ can be obtained from the equation (7),

$$\overline{h} = \frac{Nu_{HPHE}\,k}{d} \tag{7}$$

Furthermore, an expanded the surface area with plate fins into HPHE, The overall surface efficiency of a plate fin need to be derived in the hexagonal fin lay out, as shown in Figure 2. In this case, the model can be calculated by equation (8)

$$\gamma = \left(\frac{2S_T}{\sqrt{3}d} - 1\right)\left(1 + 0.35ln\left(\frac{2S_T}{\sqrt{3}d}\right)\right) \tag{8}$$

The γ is the fin parameter but the extended surface geometric parameter can be determined from $m_{es} = \sqrt{2\overline{h}/k\delta}$. Therefore, the performance of the plate fin, η_f can be calculated from the equation (9),

$$\eta_f = tanh\left(m_{es}\frac{S_T}{\sqrt{3}}\gamma\right)\Big/\left(m_{es}\frac{S_T}{\sqrt{3}}\gamma\right) \tag{9}$$

In other words, the total surface efficiency of the plate fin, η_o is used to calculate the thermal resistance of convection heat transfer as equation [21].

$$\eta_o = 1 - \frac{N_{fin}A_{fin}}{A_{HPHE}}(1 - \eta_f) \tag{10}$$

Where the N_{fin}, A_{fin} and A_{HPHE} are the number of fin, surface area of fin and surface of HPHE, respectively.

2.4 *Thermal conduction of heat pipes*

The thermal conductivity at the wall and screen wick is heated by the convection heat transfer in which hot fluids can be calculated. Actually, Heat from convection transfers to the inner surface through to screen wick, after that the boiled working fluid changes to the vapour phase and rises up to the top of heat pipes, the condensed working fluid drops by heat loss via screen wick to the evaporation zone again as Figure 3. Altogether, the thermal conductivity equation can be expressed by equation (11),

$$T_1 = \frac{\dot{q}r_1}{k}ln(\frac{r_2}{r_1}) + T_2 \tag{11}$$

Where $\dot{q}$ is the heat generation. For screen wick's thermal conductivity, $k_{l\text{-}wick}$ can be determined from below equation [22]–[24]

$$k_{l\text{-}wick} = \frac{k_l[(2k_l + k_{wick}) - (1-\varphi)(k_l - k_{wick})]}{(k_l + k_{wick}) + (1-\varphi)(k_l - k_{wick})} \quad (12)$$

Where k_l, k_{wick} and φ are the working fluid's thermal conductivity at liquid state, the material's thermal conductivity and the screen wick porosity, respectively. In this case, the porosity of the screen wick can be calculated by $\varphi = 1 - 1.05\pi. _{wick}/\varsigma$

2.5 *Thermal cycle in heat pipes*

During the working fluid is on process as Figure 3, those mathematical models are derived from the continuity equation and momentum equation as equation (1) and (2), respectively. Assumptions of the thermal cycle in heat pipes, the heat pipe's length; The evaporation's length (L_e) and condensation's length (L_c) are the same. The filling ratio of working fluid is 100% by L_e. In the process, the L_e and L_c have a liquid phase containing of 50% and vapour phase containing of 50%, respectively [25]. Thus, the length is affects to working fluid used for determination the total pressure drop, ΔP_v.

This effective length can be set as equation, $L_{eff} = 0.5L_e + L_a + 0.5L_c$. Finally, the modified equation Hagen-Poiseuille [25] of the total vapour pressure drop can be expressed as equation (13),

$$\Delta P_v = -\frac{8\mu \dot{m}_v L_{eff}}{\rho \pi R_v^4} - \rho g \sin\phi L_{eff} \quad (13)$$

Where $\dot{m}_v$ is the working fluid flowing in vapour phase and R_v is the radius of vapour core. Determining the temperature difference caused when pressure drop along heat pipe, It can be determined the relationship by the Gibbs-Duhem relation with the chemical potential form, $d\beta = -SdT + VdP$. Furthermore, the pressure gradient, $\partial P/\partial T = -(s_l - s_v)/(v_l - v_v)$, the Clausius equation, $\delta_{qint,rev} = Tds$, the entropy equation, $ds = dh/T - vdP/T$ and the equation of state, $Pv = RT$ are used for derivation with the Clausius–Clapeyron relation, $ds = gh/T$ in order to determine the temperature different, ΔT. As already mentioned, it will have temperature dropped along heat pipe as shown by equation (14),

$$\Delta T = -\frac{8\mu \dot{q} R T^2 L_{eff}}{\rho \pi h_{lv}^2 R_v^4 P} - \frac{RT^2 \rho g \sin\phi L_{eff}}{h_{lv} P} \quad (14)$$

Where the S is the entropy and the V is the volume. The s, s_l, s_v are the entropy per unit mass, the entropy per unit mass in liquid phase and the entropy per unit mass in vapour phase, respectively. The v_l, v_v, are the specific volume in liquid phase and vapour phase, respectively. The $q_{int,rev}$ is the total heat transfer during an internally reversible process per unit mass. Next, the h is enthalpy and the R is the gas constant. Equation (14) can be used to determine the thermal resistance by temperature dropped along heat pipe further. Overview, the total thermal resistance, R_{total}, as Figure 3 can be expressed as equation (15),

$$R_{total} = R_{conv,e} + \left(\begin{array}{l} \dfrac{1}{R_{cond,e} + R_{wick,e}} + \dfrac{1}{R_{axial}} \\ +R_{vapor,HP} + R_{wick,c} \\ +R_{cond,c} \end{array} \right)^{-1} + R_{conv,c} \quad (15)$$

Where R_{axial}, $R_{cond,c}$, $R_{cond,e}$, $R_{conv,c}$, $R_{conv,e}$, $R_{wick,c}$, $R_{wick,e}$ and $R_{vapor,HP}$ are the thermal resistance of container in axial, thermal resistance of radial conduction of solid wall at condensation zone, a thermal resistance of radial conduction of solid wall at evaporation zone, thermal resistance due to convection from cold fluid at condensation zone, thermal resistance due to convection from hot fluid at evaporation zone, thermal resistance of wick structure at condensation zone, thermal resistance of wick structure at evaporation zone and the thermal resistance occurring at the vapour-liquid interface, respectively

2.6 *The effectiveness of HPHE*

In the case of fluids have flowing to the staggered arrangement heat pipes, the surface temperatures of heat pipe (T_s) in either evaporation or condensation, are uniformed. Then, the log mean temperature different can be estimated by equation (16),

$$T_{out} = T_s - (T_s - T_{in}) exp\left(-\frac{A_{HPHE}\overline{h}}{\rho_f u_m (YZ - N_{fin}\delta Z_{fin}) c_{p,f}} \right) \quad (16)$$

Where T_{in}, T_{out} are the inlet and outlet temperature., and the subscript f is the fluid type. Next, the Y and Z

are the high and wide of channel for evaporation zone or condensation zone, respectively. For the δ and Z_{fin} are the fin's thickness and the fin's width. In the effectiveness of the HPHE can be determined by equation (17),

$$\varepsilon = \frac{C_h(T_{h,in} - T_{h,out})}{C_{min}(T_{h,in} - T_{c,in})} = \frac{C_c(T_{c,out} - T_{c,in})}{C_{min}(T_{h,in} - T_{c,in})} \quad (17)$$

Where C_h and C_c are the heat capacity rates of the hot air and the cold water, respectively. The C_{min} is minimum heat capacity rate.

3 Computational Procedure

The hypothesis of the analysis governing equations are calculated based on hot air and water flowing at a steady state without heat loss to the surroundings. There is also no kinematic energy, potential energy, thermal resistance occurring at the vapour-liquid interface, axial thermal resistance of wick and solid wall as well as uniform surface temperature of the heat pipes. The calculation starts from the input parameters consisting of the physical HPHE, the properties of hot air, cold water, the working fluid and working conditions. Next, calculate the thermal resistance of container in axial, thermal resistance of radial conduction of solid wall at condensation zone, a thermal resistance of radial conduction of solid wall at evaporation zone, thermal resistance due to convection from cold fluid at condensation zone, thermal resistance due to convection from hot fluid at evaporation zone, thermal resistance of wick structure at condensation zone and thermal resistance of wick structure at evaporation zone. After that, make guessed the value of the heat transfer rate ($\dot{q}$) to enter the system used for the thermal resistance of vapour dropped along heat pipe. Then combined with the thermal resistance was calculated previously. To find the new value ($\dot{q}$) until the error of ≤ 0.001. Then the values ($\dot{q}$) will be applied to calculate values of surface temperature at condensation zone and surface temperature evaporation zone. All in all, the process is shown on the Figure 4. The results of this simulation are verified with the research of H. Zare Aliabadi *et al.* [1]. Especially, in the conditions that values temperature of the hot air flowing into the evaporation zone of 398.15K and the water temperature entering to condensation zone of 290.15K used to compare

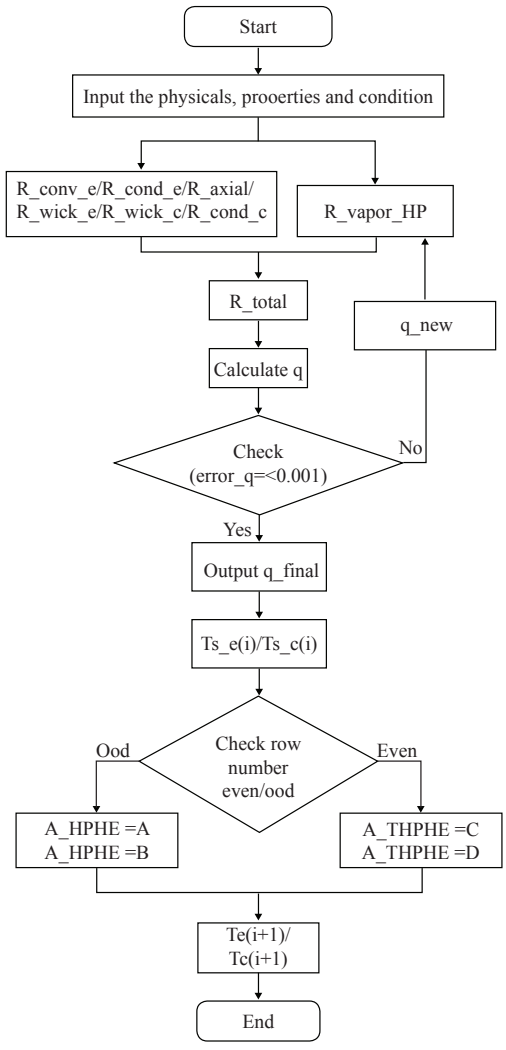

Figure 4: The steps to calculate the heat pipe with MATLAB in each row.

with the results of analytical models. The results are reported as follows; the temperature of the evaporator are likely to find that the same direction in the temperature for outlet hot air as shown in Figure 5. However, when the hot air heat capacity rates to water heat capacity rates (C^*) and the hot air temperature inlet increasing, the hot air temperature outlet increases as well. The lowest temperature outlet is at the $C^* = 0.42$ but the highest temperature outlet is at $C^* = 1.266$. From the verification results show that the analytical models differs from the simulation in the lower 3.70%, and differs from the experiments 3.04% in the higher, respectively.

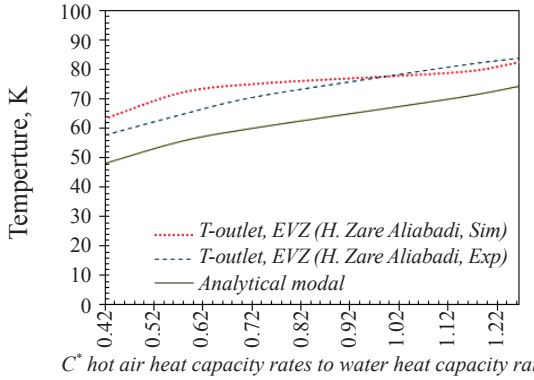

Figure 5: The comparison of the temperature for outlet hot air in the evaporation zone.

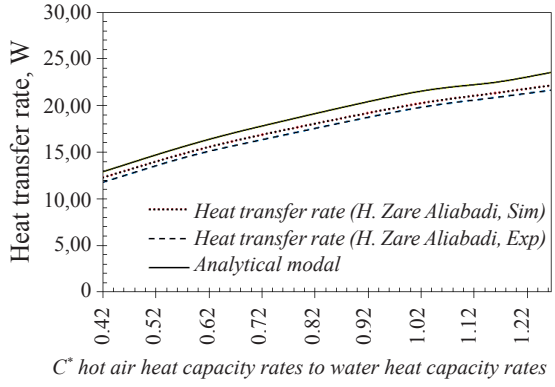

Figure 6: The comparison of the heat transfer rate in evaporation zone.

Comparison of heat transfer rate as in Figure 6 shows the trend that is similar to the verifying research when the C^* is increased, the heat transfer rate increase as well. As the matter of fact, the results of analytical models show the range from 12,917 to 23,511 Watt. Then, the analytical model differs from the simulation of H. Zare Aliabadi's results in higher at 5.38% as well as it differs from the experiment of H. Zare Aliabadi in higher at 7.89%.

The Figure 7 shows that the effectiveness is similar to H. Zare Aliabadi's results. At $C^* = 1.0$, the effectiveness is the lowest at 0.42, but the $C^* > 1.0$ carry out the effectiveness increasing again. Thus, the theoretical models differ from the simulation of H. Zare Aliabadi's results in higher at 5.66%, and differ from the experiment of H. Zare Aliabadi in higher at 8.20%. The results verify that the three most likely the work of H. Zare Aliabadi's results. However, the

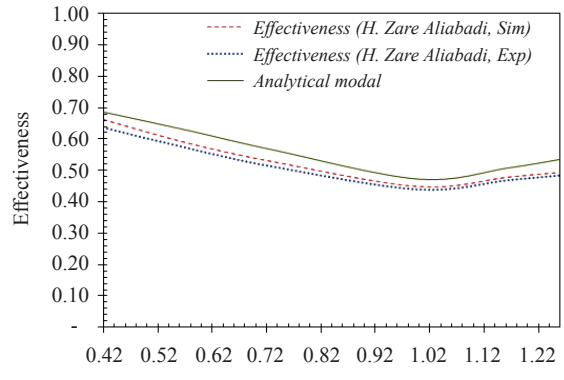

Figure 7: The comparison of the effectiveness.

staggered arrangement of HPHE is more effectiveness than the in-line arrangement, ensuring that the analytical model can be applied to other materials, and other conditions appropriately.

4 Results and Discussions

After the analytical models verified with H. Zare Aliabadi's results as topic 3. The HPHE is experimented as the topic 2.2 that hot air temperature range is 423.15 to 473.15K.

4.1 *Temperature distributions*

The experiment shows the results of the temperature distributions at 423.15, 448.15, 473.15 and 498.15K, respectively. By considering the temperature of the water outlet from condensation zone, it's increasing rapidly at the rows of 1 to 3, the temperatures are increased an average of 4.52% but the rows of 4 to 6, and it would have increased an average of 2.13%. In addition, when the temperature is increased each range such as 423.15 to 448.15K, 448.15 to 473.15K and 473.15 to 498.15K, which found that the percentage increase was 3.33%, 3.51% and 3.31% respectively. Therefore, it would be the best temperature is 473.15K, which is the highest temperature increased, as shown in Figure 8 and Figure 9. In addition, the temperature is 498.15K and the $C^* = 1.50$ gives the best temperature for water outlet increased from 303.15 to 389.50K, which is an increase of 28.48%, as shown in Figure 10 to Figure 11.

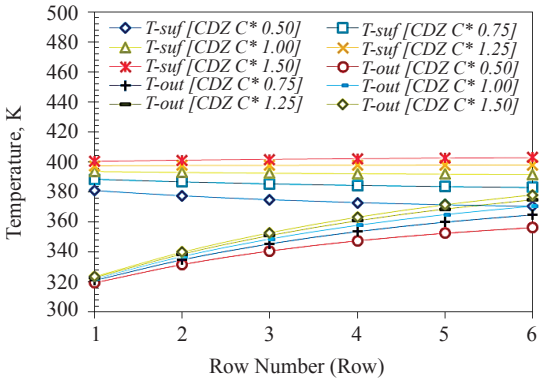

Figure 8: The temperature distribution of the surface temperature and the condenser section outlet at each of row into the air temperature is 473.15K.

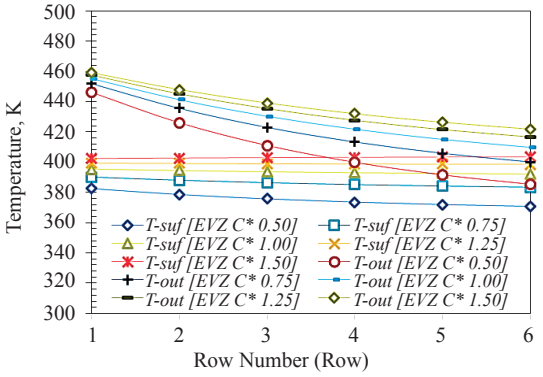

Figure 9: The temperature distribution of the surface temperature and the evaporator zone outlet at each of row into the air temperature is 473.15K.

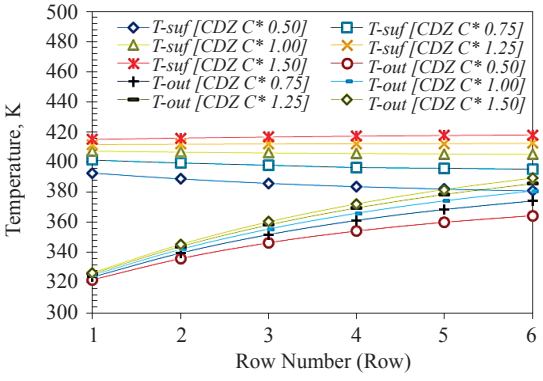

Figure 10: The temperature distribution of the surface temperature and the condenser zone outlet at each of row into the air temperature is 498.15K.

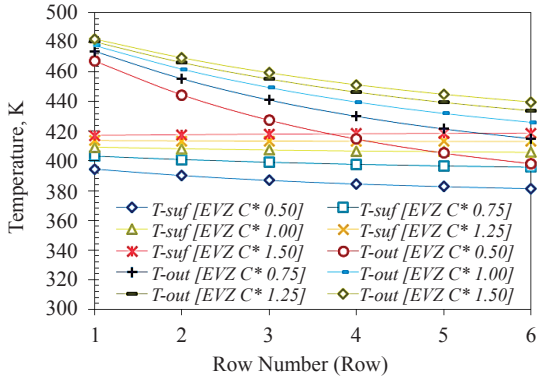

Figure 11: The temperature distribution of the surface temperature and the evaporator zone outlet at each of row into the air temperature is 498.15K.

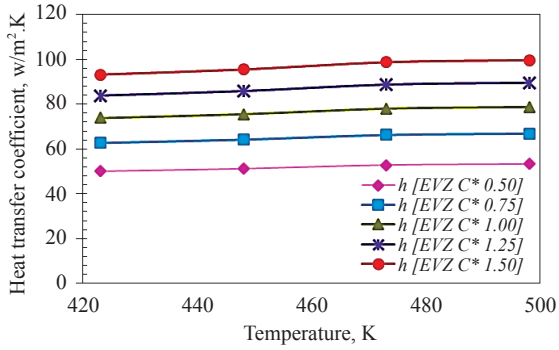

Figure 12: The heat transfer coefficient of hot air at evaporator zone.

4.2 *Heat transfer coefficient*

For the heat transfer coefficients of HPHE are shown that the temperature range of 423.15 to 498.15K and the C^* is in the range of 0.50 to 1.50 will be obtained the heat transfer coefficient values in the range of 50.07 to 99.66 W/m^{2}K, as shown on Figure 12.

4.3 *Heat output at condensation zone*

Considering the heat flux from the condenser zone, the Figure 13 shows that the temperatures for inlet hot air of 423.15 to 498.15K and the C^* is in the range of 0.50 to 1.50 will be obtained the heat flux range of 8,687.5 to 23,226.0 W/m^2. Moreover, the comparison for the ratio of C^* from current state to next state, 0.75/0.50, 1.00/0.75, 1.25/0.75 and 1.50/1.25 provide the heat

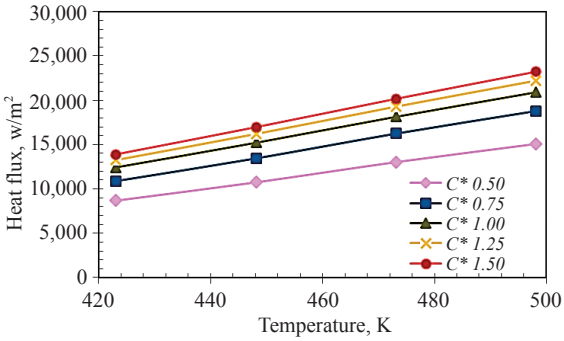

Figure 13: The heat flux in the condensation zone.

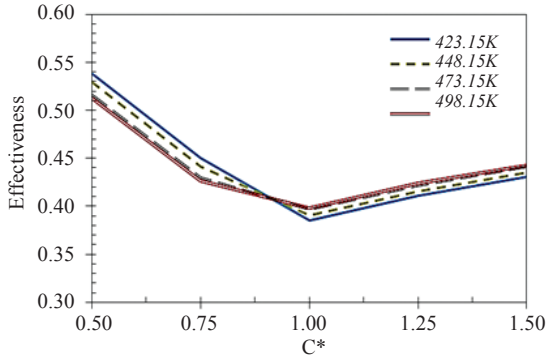

Figure 14: The effectiveness of HPHE.

flux increasing by 24.95%, 12.57%, 6.43% and 4.68%, respectively.

4.4 *Effectiveness of HPHE*

The effectiveness as shown in Figure 14 found that if the C^* increase the value, then the effectiveness decreased until $C^* = 1.0$, which the lowest is 0.39 to 0.40, and they increased again at $C^* > 1.0$. However, The overall effectiveness of the C^* range of 0.50 to 0.75 which give the best effectiveness with the temperatures for the inlet hot air of 423.15K equal to 0.54 and 0.45 respectively. In contrast the C^* range of 1.00 to 1.50 which give the best effectiveness with the temperatures for inlet hot air of 498.15K equal to 0.40, 0.42 and 0.44, respectively.

5 Conclusions

This study has shown that the analytical models used in the simulation of HPHE by using ethanol as the working fluid which are intended to apply in the waste heat recovery from exhaust gas. The results show that the hot air flowing have an air temperature of 498.15K and the $C^* = 1.50$ give the best of temperature distribution and the maximum heat transfer coefficient of 99.66 W/m^2.K as well as the heat flux occurring at a condensation zone is 23.226 W/m^2. In contrast, when the $C^* = 0.50$ is a value that makes the best effectiveness in each of the inlet hot air temperature. In particular, these mathematical models can be used for designation in further.

Acknowledgments

This research is supported by ES-MVC, Science and Technology Research Institute, Department of Mechanical and Aerospace Engineering, Faculty of Engineering, King Mongkut's University of Technology North Bangkok (KMUTNB)

References

[1] H. Zare Aliabadi, H. Ateshi, S. H. Noei, and M. Khoram, "An experimental and theoretical investigation on thermal performance of a gas-liquid thermosyphon heat pipe heat exchanger in a semi-industrial plant," *Iranian Journal Chemical Engineering*, vol. 6, no. 3, pp.13–15, summer. 2009.

[2] R. Laubscher and R. T. Dobson, "Theoretical and experimental modelling of a heat pipe heat exchanger for high temperature nuclear reactor technology," *Applied Thermal Engineering*, vol. 61, pp. 259–267, Jul. 2013.

[3] H. Mroue, J. B. Ramos, L. C. Wrobel, and H. Jouhara, "Experimental and numerical investigation of an air-to-water heat," *Applied Thermal Engineering*, vol. 78, pp. 339–350, Jan. 2015.

[4] T. S. Jadhava and M. M. Leleb, "Theoretical energy saving analysis of air conditioning system using heat pipe heat exchanger for Indian climatic zones," *Engineering Science and Technology*, vol. 18, pp. 669–673, Dec. 2015.

[5] H. Chaoling and Z. Linjiang, "Study on the heat transfer characteristics of a moderate-temperature heat pipe heat exchanger," *International Journal of Heat and Mass Transfer*, vol. 91, pp. 302–310, Dec. 2015.

[6] A. El-Baky, A. Mostafa, and M. M. Mousa, "Heat pipe heat exchanger for heat recovery in air conditioning," *Applied Thermal Engineering*, vol. 27, pp. 795–801, 2007.

[7] A. L. Giovanni, G. Righetti, C. Zilio, and F. Bertolo, "Experimental and theoretical analysis of a heat pipe heat exchanger operating with a low global warming potential refrigerant," *Applied Thermal Engineering*, vol. 65, pp. 361–368, Jan. 2014.

[8] S. L. Tian and M. H. Yew, "Experimental investigation on the thermal performance and optimization of heat sink with U-shape heat pipes," *Energy Conversion and Management*, vol. 51, pp. 2109–2116, Apr. 2010.

[9] H. Mrouea, J. B. Ramosa, L. C. Wrobelb, and H. Jouharaa, "Experimental and numerical investigation of an air-to-water heat pipe-based heat exchanger," *Applied Thermal Engineering*, vol. 78, pp. 339–350, Mar. 2015.

[10] Y. Feng, Y. Xiugan, and L. Guiping, "Waste heat recovery using heat pipe heat exchanger for heating automobile using exhaust gas," *Applied Thermal Engineering*, vol. 23, pp. 367–372, Oct. 2002.

[11] R. Saidura, M. Rezaeia, W. K. Muzammila, M. H. Hassana, S. Pariaa, and M. Hasanuzzaman, "Technologies to recover exhaust heat from internal combustion engines," *Renewable and Sustainable Energy Reviews*, vol. 6, pp. 5649–5659, May. 2012.

[12] A. Meyer and R. T. Dobson, "A heat pipe heat recovery heat exchanger for a mini-drier," *Journal of Energy in Southern Africa*, vol. 17, no. 1, Feb. 2006.

[13] K. Hiroaki, I.Hideaki, and I. Yuji, "The permeability of screen wicks," *The Japan Society of Mechanical Engineers*, vol.34, no.2, 1991.

[14] C. Wang , B. He, L. Yan , X. Pei, and S. Chen, "Thermodynamic analysis of a low-pressure economizer based waste heat recovery system for a coal-fired power plant," *Energy*, vol. 65, pp. 80–90, Feb. 2014.

[15] C. Wang, B. He, S. Sun, Y. Wu, N. Yan, L. Yan, and X. Pei, "Application of a low pressure economizer for waste heat recovery from the exhaust flue gas in a 600 MW power plant," *Energy*, vol. 48, pp. 196–202, Dec. 2012.

[16] S. Niamsuwana, P. Kittisupakorna, and I. M. Mujtabab," A newly designed economizer to improve waste heat recovery: A case study in a pasteurized milk plant," *Applied Thermal Engineering*, vol. 60, pp. 188–199, Oct. 2013.

[17] G. K. James and L. K. Donald, "Fluid dynamics and Heat transfer," *Chemical Engineering Series*, New York: McGraw-Hill, 1958, pp. 23–43.

[18] W. A. Khan, J. R. Culham, and M. M. Yovanovich, "Convection heat transfer from tube banks in crossflow: Analytical approach," *International Journal of Heat and Mass Transfer*, vol. 49, pp. 4831–4838, Aug. 2006.

[19] V. K. Mandhani, R. P. Chhabra, and V. Eswaran, "Forced convection heat transfer in tube banks in cross flow," *Chemical Engineering Science*, vol. 57, pp. 379–391, Aug. 2001.

[20] M. B. Brenda, B. G. Judith, L. Lackenbach, and M. Gonzalez, "Heat exchanger design handbook," *Heat and Mass Transfer*, vol. 1, New York: BookCrafters, Inc., 1983, pp. 2.5.2-1–2.5.7-31.

[21] F. W. Monifa, "Plate – fin and- tube condenser design for refrigerant R-410 Air-conditioner," M.S. thesis, Department of Science in Mechanical Engineering, Georgia Institute of Technology Log, May. 2000.

[22] T. Sheng-Hong, C. Yu-Tang, and K. Shung-Wen, "Fabrication of composite wick structure heat spreader," *Journal of Marine Science and Technology*, vol. 20, pp. 158–162, 2012.

[23] A. B. Solomon, K. Ramachandran, L. G. Asirvatham, and B. C. Pillai, "Numerical analysis of a screen mesh wick heat pipe with Cu/water nanofluid," *International Journal of Heat and Mass Transfer*, vol. 75, pp. 523–533, May. 2014.

[24] J. Le-lun, T. Yong, Z. Wei, J. Lin-zhen, X. Tan, L. Yan, and G. Jin-wu, "Design and fabrication of sintered wick for miniature cylindrical heat pipe," *Transactions of Nonferrous Metals Society of China*, vol. 24, pp. 292–301, Jun. 2004.

[25] D. A. Reay and P. A. Kew, "Heat pipes theory design and application," *Science & Technology Rights*, 5nd ed, Great Britain: Elsevier, 2006, pp. 29–54